TECHNICAL REPORT
NATICK/TR-08/004

AD_____

RESOURCE-EFFICIENT DIGITAL COMMUNICATIONS: RESEARCH AND TESTBED DEVELOPMENT IN SUPPORT OF FUTURE FORCE WARRIOR AND JOINT TACTICAL RADIO SYSTEMS

by
Thomas Fuja
Oliver Collins
Daniel Costello, Jr.
and
Yih-Fang Huang

University of Notre Dame
Notre Dame, IN 46556

November 2007

Final Report
August 2002 – December 2006

Approved for public release; distribution is unlimited

Prepared for
U.S. Army Natick Soldier Research, Development and Engineering Center
Natick, Massachusetts 01760-5056

DISCLAIMERS

The findings contained in this report are not to be construed as an official Department of the Army position unless so designated by other authorized documents.

Citation of trade names in this report does not constitute an official endorsement or approval of the use of such items.

DESTRUCTION NOTICE

For Classified Documents:

Follow the procedures in DoD 5200.22-M, Industrial Security Manual, Section II-19 or DoD 5200.1-R, Information Security Program Regulation, Chapter IX.

For Unclassified/Limited Distribution Documents:

Destroy by any method that prevents disclosure of contents or reconstruction of the document.

REPORT DOCUMENTATION PAGE

Form Approved
OMB No. 0704-0188

1. REPORT DATE *(DD-MM-YYYY)*	2. REPORT TYPE	3. DATES COVERED *(From - To)*
28-11-2007	Final	August 2002 to December 2006

4. TITLE AND SUBTITLE
RESOURCE-EFFICIENT DIGITAL COMMUNICATIONS: RESEARCH AND TESTBED DEVELOPMENT IN SUPPORT OF FUTURE FORCE WARRIOR AND JOINT TACTICAL RADIO SYSTEMS

5a. CONTRACT NUMBER
DAAD16-02-C-0057

5b. GRANT NUMBER

5c. PROGRAM ELEMENT NUMBER

6. AUTHOR(S)
Thomas Fuja, Oliver Collins, Daniel Costello, Jr., and Yih-Fang Huang

5d. PROJECT NUMBER

5e. TASK NUMBER

5f. WORK UNIT NUMBER

7. PERFORMING ORGANIZATION NAME(S) AND ADDRESS(ES)
University of Notre Dame
Department of Electrical Engineering
275 Fitzpatrick Hall
Notre Dame, IN 46556

8. PERFORMING ORGANIZATION REPORT NUMBER

9. SPONSORING/MONITORING AGENCY NAME(S) AND ADDRESS(ES)
U.S. Army Natick Soldier Research, Development and Engineering Center (NSRDEC)
ATT'N: AMSRD-NSF-TP-S (Henry Girolamo)
Kansas Street
Natick, MA 01760-5056

10. SPONSOR/MONITOR'S ACRONYM(S)

11. SPONSORING/MONITORING AGENCY REPORT NUMBER
NATICK/TR-08/004

12. DISTRIBUTION AVAILABILITY STATEMENT
Approved for public release; distribution is unlimited.

13. SUPPLEMENTARY NOTES

14. ABSTRACT
This report describes the design and simulation of a bandwidth-efficient waveform suitable for the SLICE radio developed by ITT Aerospace/Communications; this waveform uses quadrature amplitude modulation (QAM) and low-complexity turbo codes developed at Notre Dame. The result is compared with another using continuous phase modulation (CPM). It is shown that the amplifier backoff required for QAM puts it at a disadvantage to CPM at spectral efficiencies where both are feasible - below 2.0 bits/sec/Hz. However, signal processing techniques (e.g., pre-distortion filtering) for QAM can reduce that disadvantage; moreover, at higher spectral efficiencies, QAM may be the only feasible solution. Other topics include low-density parity check (LDPC) convolutional codes, new techniques to reduce the peak to average power ratio (PAPR) for QPSK signals, and analysis of systems employing adaptive modulation and orthogonal frequency division multiplexing (OFDM).

15. SUBJECT TERMS

SPECTRA	BANDWIDTH	FREQUENCY HOPPING	LDPC(LOW-DENSITY PARITY-CHECK)
EFFICIENCY	TURBO CODES	ERROR CONTROL CODES	JTRS(JOINT TACTICAL RADIO SYSTEM)
AMPLIFIERS	LINEAR SYSTEMS	DIGITAL COMMUNICATIONS	COMMUNICATION AND RADIO SYSTEMS
WAVEFORMS	RADIO EQUIPMENT	FFW(FUTURE FORCE WARRIER)	CPM(CONTINUOUS PHASE MODULATION)

16. SECURITY CLASSIFICATION OF:			17. LIMITATION OF ABSTRACT	18. NUMBER OF PAGES	19a. NAME OF RESPONSIBLE PERSON
a. REPORT	b. ABSTRACT	c. THIS PAGE	SAR	30	Henry Girolamo
U	U	U			19b. TELEPONE NUMBER *(Include area code)* 508-233-5483

Table of Contents

List of Figures

Preface

This report describes research activity carried out at the University of Notre Dame under U.S. Department of Defense Contract DAAD16-02-C-0057 from August 2002 through December 2006. The work was supervised by the four Notre Dame faculty members authoring this report; the team also included graduate students, post-doctoral researchers, and visiting researchers.

Resource-Efficient Digital Communications:
Research and Testbed Development in Support of FFW and JTRS

Executive Summary

The focus of this research effort has been to develop communication technology well-suited to tactical military communications generally and the FFW and JTRS programs specifically. This document describes the following:

- The design and simulation-based testing of a bandwidth-efficient transceiver suitable for implementation in the SLICE radio developed by ITT Aerospace/Communications Division. This transceiver uses novel error control coding technology developed at Notre Dame in conjunction with quadrature amplitude modulation (QAM) to deliver data at up to 3.75 bits per QAM symbol (not including pilots). The Notre Dame team also developed modules carrying out synchronization, channel estimation, and equalization. The resulting transceiver was simulated and compared with comparable results for a competing technology – continuous phase modulation (CPM). It was shown that the power amplifier backoff required for QAM puts it at a competitive disadvantage to CPM at spectral efficiencies where both are feasible – i.e., below 2.0 bits/sec/Hz. However, signal processing techniques (such as predistortion filtering) for QAM signalling are available to reduce that disadvantage; moreover, at higher spectral efficiencies, a QAM-based approach may be the *only* feasible solution.

- The development of a new class of error control codes called *low density parity check (LDPC) convolutional codes.* These are convolutional versions of LDPC block codes that are being incorporated into a variety of communication standards. It has been shown that LDPC convolutional codes have significant performance and complexity advantages over their block code counterparts.

- New techniques for reducing the peak-to-average power ratio (PAPR) for Nyquist-filtered QPSK signals. Reducing the PAPR relaxes the need for linear power amplifiers, resulting in less expensive, more power-efficient transceiver.

- Analysis of communication systems employing *adaptive modulation,* in which aspects of the transmitted signal are changed automatically depending on the quality of the communication channel. Specifically, we analyzed the effect of imperfect feedback - i.e., the effect of the transmitter getting flawed knowledge about the channel - and proposed practical schemes based on statistical communication theory.

- Development of synchronization and estimation algorithms well suited to orthogonal frequency division multiplexing (OFDM).

1 Design of Bandwidth-Effi cient Mode of Operation for the SLICE Radio Platform

1.1 Background and Motivation:

The Soldier Level Integrated Communications Environment (SLICE) is a radio developed by ITT Aerospace/Communications Division of Ft. Wayne, IN under contract to the U.S. Army. Normally, SLICE operates in a spread-spectrum mode; however, a narrowband, bandwidth-efficient mode of operation is required for training purposes. Currently, that narrowband mode of operation is based on licensed technology provided by TrellisWare, Inc. of Poway, CA. The TrellisWare approach uses a high-rate channel code in conjunction with continuous phase modulation (CPM) to effect a spectral efficiency up to slightly more than 2.0 bps/Hz.

Under this contract, Notre Dame developed an alternative bandwidth-efficient mode of operation based on quadrature amplitude modulation (QAM) and low-complexity turbo codes. The potential advantages of this approach are threefold: (1.) better noise immunity; (2.) higher possible spectral efficiency; and (3.) no requirement to pay licensing fees. The primary disadvantage of the QAM-based approach lies in its reliance on linear high-power amplifiers, which are typically less power-efficient than the non-linear amplifiers used in CPM.

This section of the report describes the Notre Dame design and compares a QAM-based approach with a CPM-based approach.

1.2 Low-Complexity Turbo Codes and QAM

The structure of a conventional turbo encoder is shown in Figure 1. In such a structure, incoming data is encoded twice - first in its original order and then again after it's been re-ordered - i.e., "permuted" or "interleaved". (Throughout this document, an interleaver is designated as a subscripted "π".) The redundant (parity) bits generated by each of the two encoders are transmitted along with the original data. An example of the turbo code used in 3G cellular systems in shown in Figure 2.

Figure 3 shows a low-complexity turbo encoder designed by Massey and Costello at Notre Dame. Notably, there are four (not two) constituent encoders, and each of the constituent encoders contains only a single memory element - i.e., they are all two-state constituent codes. The performance of these low-complexity has been shown to be superior to that of the 3GPP code [1] at lower complexity [2].

The Notre Dame design employs a low-complexity turbo encoder used in conjunction with quadrature amplitude modulation (QAM). In M-ary QAM signaling, one of $M = 2^b$ different symbols are transmitted during each symbol period, representing b bits. These M different symbols are represented as points on a two-dimensional grid; specifically, the point (s_I, s_Q) represents the signal with in-phase component s_I and quadrature component s_Q – i.e.,

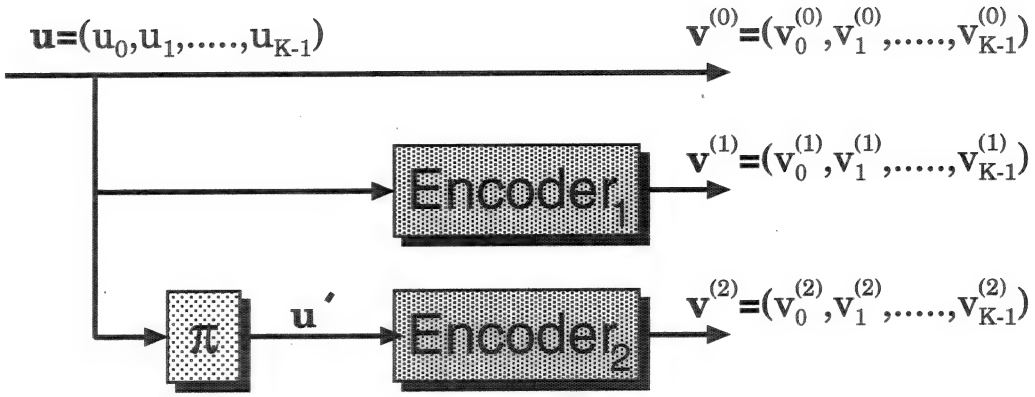

Figure 1. A conventional turbo encoder structure.

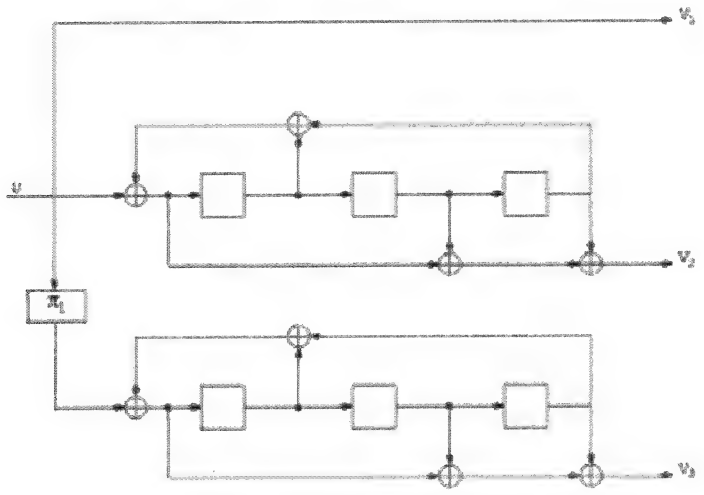

Figure 2. An example of a conventional turbo encoder - i.e., the turbo encoder used in 3G cellular systems.

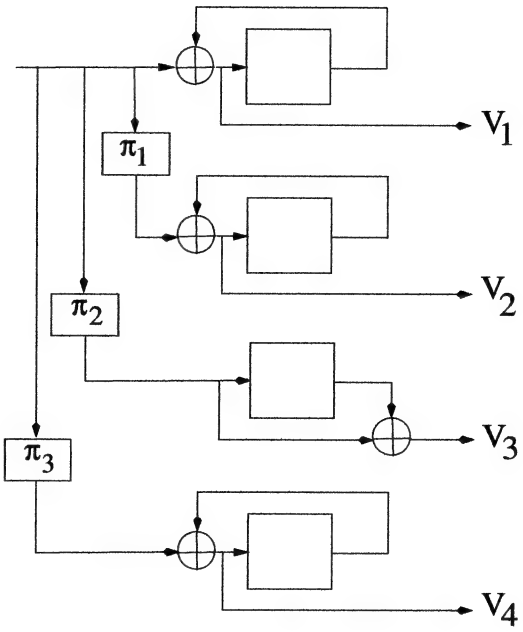

Figure 3. Low-complexity turbo encoder designed by Notre Dame team.

it represents

$$s(t) = s_I \cos(2\pi f_o t) - s_Q \sin(2\pi f_o t)$$

shifted to the appropriate time interval. (Here, f_o is the carrier frequency; moreover, $s(t)$ is typically passed through a "shaping filter" prior to transmission to reduce the bandwidth of the resulting transmitted signal.)

Figure 4 shows the output of the low-complexity turbo encoder mapped onto the 16-QAM signal set; the "puncturing pattern" indicates that encoded bits are punctured (or deleted) in three-bit blocks; the pattern "110", for instance, indicates that the first two bits are transmitted and the third is punctured. (Note that *none* of the information bits are transmitted – i.e., this is a non-systematic encoder.) With the puncturing of bits carried out as indicated, the turbo encoder in Figure 4 has a rate of $1/2$ - i.e., one information bit per two bits produced - and so the scheme shown has a spectral efficiency of 2 bits/symbol, or a nominal spectral efficiency of 2.0 bits/sec/Hz. (Note that if the shaping filter has an excess bandwidth parameter of α, then the actual spectral efficiency of M-ary QAM encoded with a rate-R code is $\gamma = R\log_2(M)/(1+\alpha)$ bits/sec/Hz; the "nominal" spectral efficiency assumes $\alpha = 0$, whereas more realistic values would be $0.1 \leq \alpha \leq 0.35$.)

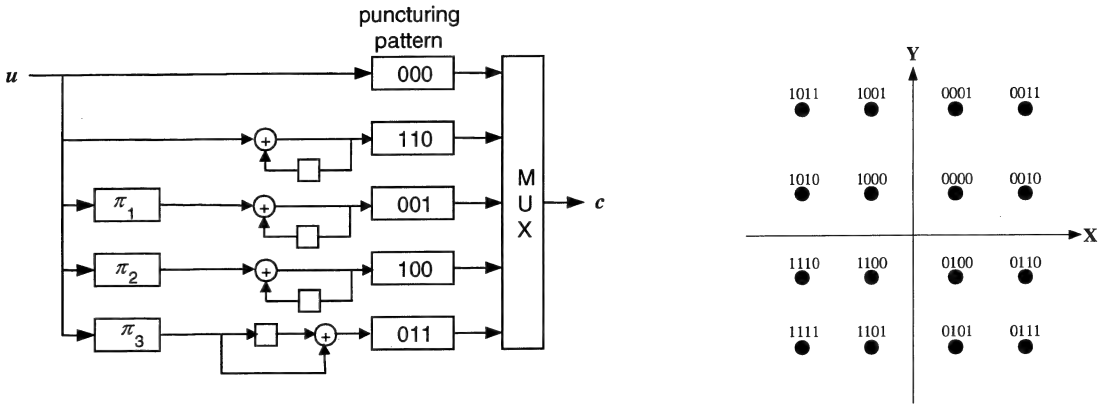

Figure 4. The low-complexity turbo encoder mapped onto 16-QAM modulation signal set.

1.3 A Description of the Proposed Architecture

A system-level description of the proposed transceiver is shown in Figure 5. It consists of the following components:

- A "channel encoder" that accepts information bits and produces code bits. An important parameter of the encoder is its rate R; if it produces n code bits for every k information bits, then it has a rate $R = k/n$. The channel encoder in the Notre Dame design is the low-complexity turbo code described in the last section with rates $R = 1/2$ and $R = 3/4$.

- A "bit interleaver" that changes the order of the bits produced by the channel encoder. (Note that this is a different interleaver that is internal to the turbo channel encoder.) The purpose of this interleaver is to "spread out" coded bits in time so that when error "bursts" occur - i.e., many errors in close temporal proximity - the effect of the burst is spread out over the coded sequence.

- A QAM mapper that takes the output of the bit interleaver and uses them to select one of $M = 2^b$ signals to transmit during the associated signaling interval. An example of this is shown in Figure 4.

- A channel that exhibits both intersymbol interference (ISI) and additive white Gaussian noise (AWGN), represented in Figure 5 by the modules labelled "Fading ISI Channel" and the adder that combined the output of that module and a random variable z, respectively.

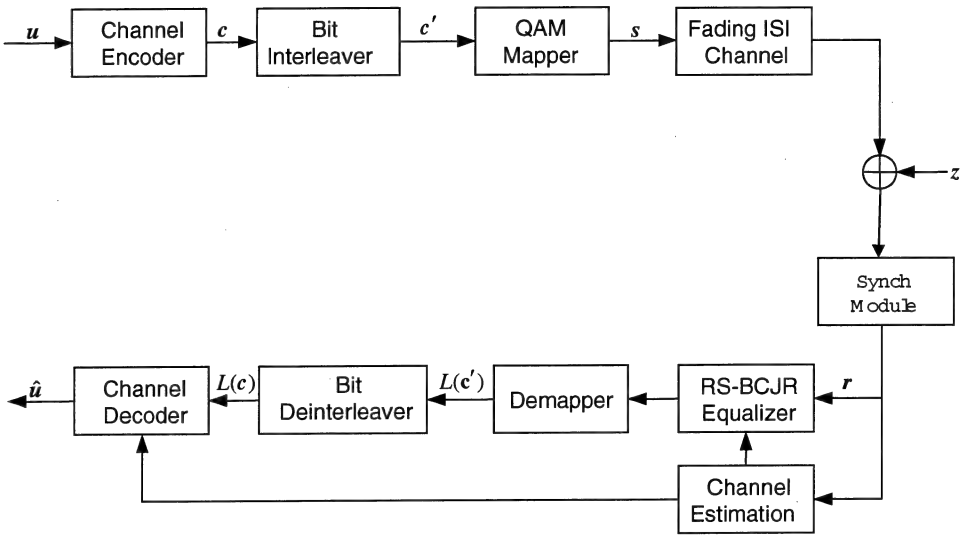

Figure 5. The low-complexity turbo encoder mapped onto 16-QAM modulation signal set.

- A synchronization module that performs both symbol-level and frame-level synchronization of the incoming signal - i.e., it uses the samples of the downconverted waveform to estimate the timing offset associated with each transmitted symbol and the boundaries of the modulated frames.
- A channel estimation algorithm that uses the "pilot" (known) symbols embedded in each frame to estimate the effect of the channel on the unknown (data-bearing) symbols in the frame.
- An equalizer that compensates for the effects of the channel, using the channel estimate provided by the channel estimation module.
- A "de-mapper" that demodulates the downconverted signal into a sequence of two-dimensional points (representing the transmitted symbols plus noise in each dimension) and produces a sequence of "soft" bit values indicating the confidence (or reliability) with which each bit has been detected.
- A bit deinterleaver that re-orders the transmitted bits into the order they were in prior to bit-interleaving.
- Finally, a channel decoder that uses the soft bit estimates and the structure provided by the turbo encoder to provide a reliable estimate of the transmitted data.

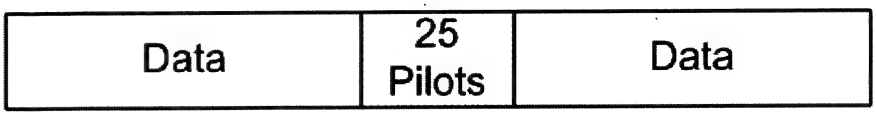

Figure 6. The hop frame structure.

1.4 A Suitable Frame Structure

To assess the performance of the proposed system, an appropriate data format was developed. Based on input from ITT engineers, a frequency-hopping architecture was assumed - i.e., one frame of data is transmitted at a particular carrier frequency, and then the next frame is transmitted at another (pseudo-randomly chosen) carrier frequency.

A frequency-hopping architecture requires that the receiver obtain synchronization and a good estimate of the channel within each frame; this in turn requires that every frame contain "pilot" symbols - i.e., symbols known in advance to both transmitter and receiver. After considerable experimentation, it was determined that 25 pilot symbols were adequate to carry out these functions, so a frame structure that embeds 25 pilot symbols in the middle of each frame was adopted. (See Figure 6.) (The pilot symbols are embedded in the *middle* of the frame because providing known information in the middle of the frame provides the best estimate of the channel out to the frame's edge.)

Each turbo codeword was transmitted over either eight or sixteen hops; this has the effect of "averaging out" the channel fading over an entire codeword. A total of eight frame structures were used:

- 8-hop and 16-hop frames for use with 16-QAM and a rate-1/2 channel code;
- 8-hop and 16-hop frames for use with 16-QAM and a rate-3/4 channel code;
- 8-hop and 16-hop frames for use with 32-QAM and a rate-1/2 channel code;
- 8-hop and 16-hop frames for use with 32-QAM and a rate-3/4 channel code.

The details of these frame structures are described in Figures 7-10. We briefly consider the contents of Figure 7:

- For both the 8-hop and 16-hop implementation, there are 8204 bits in each turbo codeword. Each turbo codeword represents 4096 data bits encoded at a rate of 1/2 with additional "tail" bits added onto the end of each codeword to drive the encoder into a known state.

Structure	8 hops	16 hops
Data/redundancy/tail bits in each turbo codeword	8204	8204
Zero padding bits	20	52
non-pilot symbols per turbo codeword	(8204+20)/4 = 2056	(8204+52)/4 = 2064
non-pilot symbols per hop	2056/8 = 257	2064/16 = 129
pilot symbols per hop	25	25
symbols per hop	284	156

Figure 7. Frame details for systems using 16-QAM modulation and rate-1/2 channel codes.

- Zeroes are padded into each frame to make each frame in an 8-hop (or 16-hop) turbo codeword the same length.
- Symbols from the 16-QAM alphabet are formed by taking four bits at a time to form a single 16-ary symbol. The result are 257 (129) 16-ary symbols in each of the eight (sixteen) hops making up one codeword.
- Each frame is loaded with 25 pilot symbols, as described above. Finally, two additional symbol durations are added to each frame to provide time for synchronization. The net result is $257 + 25 + 2 = 284$ $(129 + 25 + 2 = 156)$ symbols in each frame.

1.5 Simulations - Model Description and Performance Results

Three static channel models were provided by ITT Aerospace/Communications; they are described in Figure 11. For example, Channel 1 describes a multipath channel with three path components - a primary (reference) component, a secondary component with received power that is 2 dB below the primary component and trails it by 0.2 μs, and a tertiary component that is 10 dB below the primary component and trails it by 0.4 μs. Similarly, Channels 2 and 3 have five and six path components, respectively. The channels are "static" in that Rayleigh fading is applied to each path but the fading is constant over a single hop (frame); that is, the channel does not change appreciably during the time required to transmit a single frame - a reasonable assumption for the frame rates and mobility assumptions being made.

Structure	8 hops	16 hops
Data/redundancy/tail bits in each turbo codeword	5474	5474
Zero padding bits	30	30
non-pilot symbols per turbo codeword	(5474+30)/4 = 1376	(5474+30)/4 = 1376
non-pilot symbols per hop	1376/8 = 172	1376/16 = 86
pilot symbols per hop	25	25
symbols per hop	199	113

Figure 8. Frame details for systems using 16-QAM modulation and rate-3/4 channel codes.

Structure	8 hops	16 hops
Data/redundancy/tail bits in each turbo codeword	8204	8204
Zero padding bits	36	36
non-pilot symbols per turbo codeword	(8204+36)/5 = 1648	(8204+36)/5 = 1648
non-pilot symbols per hop	1648/8 = 206	1648/16 = 103
pilot symbols per hop	25	25
symbols per hop	233	130

Figure 9. Frame details for systems using 32-QAM modulation and rate-1/2 channel codes.

Structure	8 hops	16 hops
Data/redundancy/tail bits in each turbo codeword	5474	5474
Zero padding bits	6	46
non-pilot symbols per turbo codeword	(5474+6)/5 = 1096	(5474+46)/5 = 1104
non-pilot symbols per hop	1096/8 = 137	1104/16 = 69
pilot symbols per hop	25	25
symbols per hop	166	96

Figure 10. Frame details for systems using 32-QAM modulation and rate-3/4 channel codes.

	Path	Delay w.r.t Path1(usec)	Loss w.r.t Path 1(dB)
Channel #1	1	0	0
	2	0.2	-2
	3	0.4	-10
Channel #2	1	0	0
	2	0.2	-2
	3	0.4	-4
	4	0.6	-7
	5	2.9	-6
Channel #3	1	0	0
	2	0.2	+3
	3	0.5	-2
	4	1.6	-6
	5	2.3	-8
	6	2.9	-10

Figure 11. Descriptions of the three static channel models provided to Notre Dame by ITT Aerospace/Communications Division.

					Not including pilots		Including pilots		
Constellation	Code Rate	Code	Hops per Codeword	non-pilots per hop	Info bits per QAM symbol	Info bits/sec per Hz (α=0.25)	Info bits/sec sec per Hz	KBPS in 25 kHz slot	Pilot Energy Penalty (dB)
16-QAM	1/2	3GPP	8	263	2	1.6	1.40	35.1	1.86
16-QAM	1/2	3GPP	16	135	2	1.6	1.25	31.2	3.11
16-QAM	1/2	2-state	8	263	2	1.6	1.40	35.1	1.86
16-QAM	1/2	2-state	16	135	2	1.6	1.25	31.2	3.11
16-QAM	3/4	3GPP	8	167	3	2.4	1.98	49.5	2.66
16-QAM	3/4	3GPP	16	87	3	2.4	1.69	42.3	4.11
16-QAM	3/4	2-state	8	167	3	2.4	1.98	49.5	2.66
16-QAM	3/4	2-state	16	87	3	2.4	1.69	42.3	4.11
32-QAM	1/2	3GPP	8	212	2.5	2	1.70	42.5	1.33
32-QAM	1/2	3GPP	16	109	2.5	2	1.48	37.1	2.34
32-QAM	1/2	2-state	8	212	2.5	2	1.70	42.5	1.33
32-QAM	1/2	2-state	16	109	2.5	2	1.48	37.1	2.34
32-QAM	3/4	3GPP	8	135	3.75	3	2.38	59.53	1.87
32-QAM	3/4	3GPP	16	71	3.75	3	1.97	49.23	3.16
32-QAM	3/4	2-state	8	135	3.75	3	2.38	59.53	1.87
32-QAM	3/4	2-state	16	71	3.75	3	1.97	49.23	3.16

Figure 12. List of code/modulation configurations that were simulated.

Figure 12 describes the 16 different code/modulation combinations that were simulated under this project. They range in spectral efficiency from 1.40 bits/sec/Hz to 2.38 bits/sec/Hz when the effects of all redundancy – error control coding plus pilots - is included.

For comparison, we used bandwidth-efficient continuous phase modulation (CPM) schemes as proposed by Chugg *et al.* [3, 4]. This is accomplished by increasing the length of the phase pulse (thereby introducing intersymbol interference) and reducing the modulation index; the net result is an increase in spectral efficiency at the cost of increased complexity.

The various bandwidth-efficient modes of operation were compared at the same frame error rate of 1% – an operating point suggested by engineers at ITT Aerospace/Communications Division. (There is typically another high-layer ARQ protocol implemented on top of the physical-layer error control described here. When a frame error occurs – which will occur in 1% of the frames – the higher layer protocol requests a re-transmission of the affected frame.)

We generated two different sets of results for the turbo-QAM design - one that takes into account the power efficiency loss incurred due to the backoff required for the power amplifier to work in a linear region. To take this power loss into account, a travelling wave tube (TWT) amplifier model with strong AM/PM conversion was employed [5]. This model assumes that an input signal with envelope $\rho(t)$ produces an output signal with envelope

$$A[\rho(t)] = A_{sat}^2 \frac{\rho(t)}{\rho^2(t) + A_{sat}^2}$$

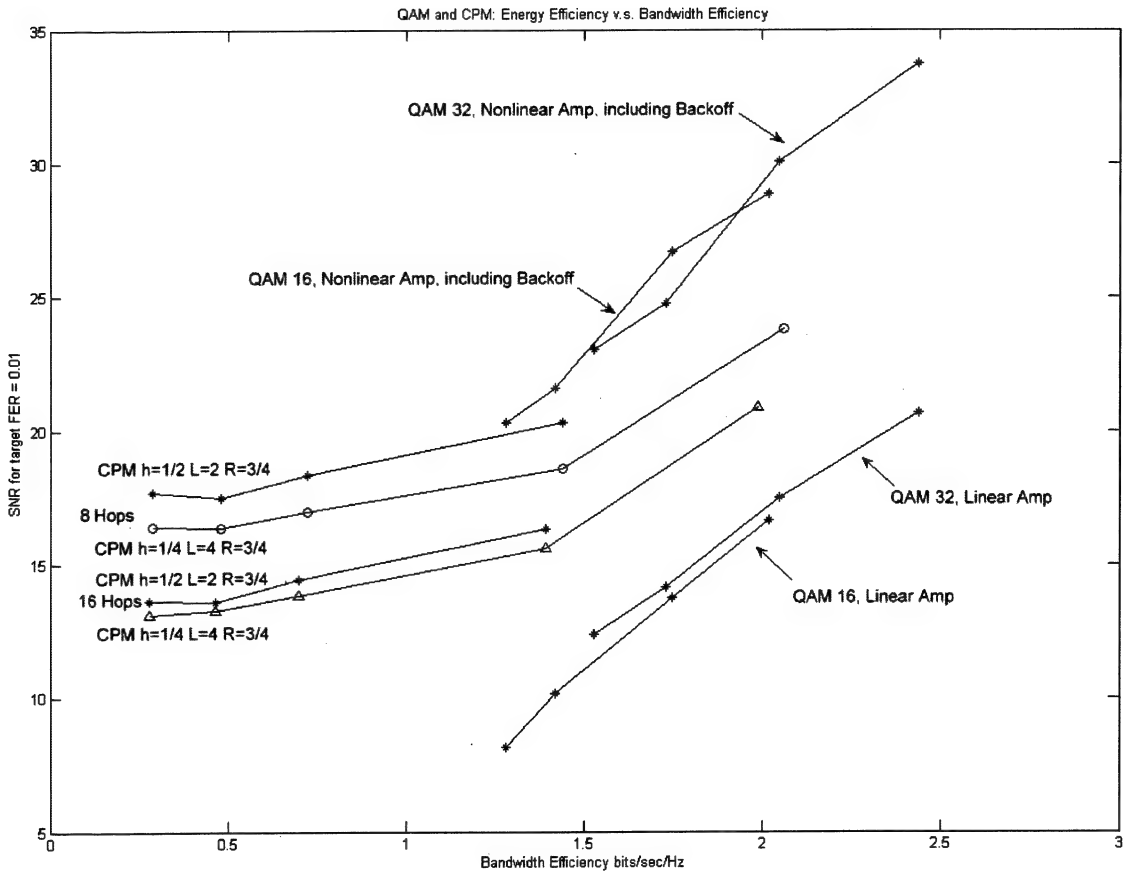

Figure 13. Comparison of turbo-coded QAM and CPM approach to bandwidth-efficient communication.

and phase

$$\Phi[\rho(t)] = \frac{\pi}{3} \frac{\rho^2(t)}{\rho^2(t) + A_{sat}^2}.$$

The simulation results are summarized in Figure 13. Each code/modulation combination is characterized by a spectral efficiency (on the x-axis) and a signal-to-noise ratio (E_b/N_0) required to obtain a frame error rate of 1% (on the y-axis). The points labelled "linear amp" assume that a linear high-power amplifier with no power penalty is available; those labelled "nonlinear amp, including backoff" make a more realistic assumption – that linear amplification is obtained by incurring a "backoff" penalty with a nonlinear amplifier.

The following observations can be made regarding the simulation results:

- Turbo-coded QAM represents a way to increase spectral efficiency on the communi-

cation channels of interest above the (approximately) 2.0-2.5 bits/sec/Hz that can be provided by CPM. Indeed, with higher rate turbo codes (and QAM constellations of 64 points or more), spectral efficiencies of 3.5 bits/sec/Hz are possible.

- The penalty paid for amplifier backoff in QAM is substantial – as much as 12 dB under our model – and can tip the balance between QAM and CPM at spectral efficiencies where both are potentially viable.

- There are signal processing techniques – for example, predistortion filtering, in which the signal is distorted prior to amplification to compensate for the nonlinear effects of amplification – that can "buy back" (with increased complexity costs) some of the power penalty assumed for nonlinear amplifiers in Figure 13. Employing such techniques could make turbo-coded QAM more competitive with CPM at spectral efficiencies below 2.5 bits/sec/Hz.

2 Other Supported Research Projects

While the bandwidth-efficient mode for SLICE was the focal point of the Notre Dame/ITT collaboration, it was not the only research supported under award DAAD16-02-C-0057. In this section, we briefly describe four other projects that were carried out with this funding.

2.1 LDPC Convolutional Codes

Capacity-approaching code designs, such as turbo codes and low-density parity-check (LDPC) codes, along with iterative message-passing decoding, can be combined with quadrature amplitude modulation (QAM) using bit-interleaved coded modulation (BICM) to provide highly reliable, power- and bandwidth-efficient waveforms for SLICE- and FFW-type radio platforms. As an alternative to the more conventional turbo codes and LDPC block codes, we have also investigated the use of LDPC convolutional codes, which have several potential advantages compared to the standard approaches. Our research in this area has been published widely in leading technical journals and conference proceedings [6, 7, 8, 9, 10, 11, 12]. Here we briefly summarize some of the more recent aspects of this research.

In [13], we introduced a technique for "unwrapping" regular quasi-cyclic LDPC block codes (QCLDPC-BCs) to form regular LDPC convolutional codes (LDPC-CCs). In that paper, we used an unwrapping technique that resulted in a time-invariant LDPC-CC with a significant "convolutional gain" compared to the underlying QCLDPC-BC. For example, a 0.9dB gain at a BER of 10^{-5} was obtained for a rate 2/5 LDPC-CC obtained by unwrapping a [155,64] QCLDPC-BC. The decoding graph representation of the two codes is essentially the same, with the LDPC-CC graph being obtained by replicating the QCLDPC-BC graph in time. Thus

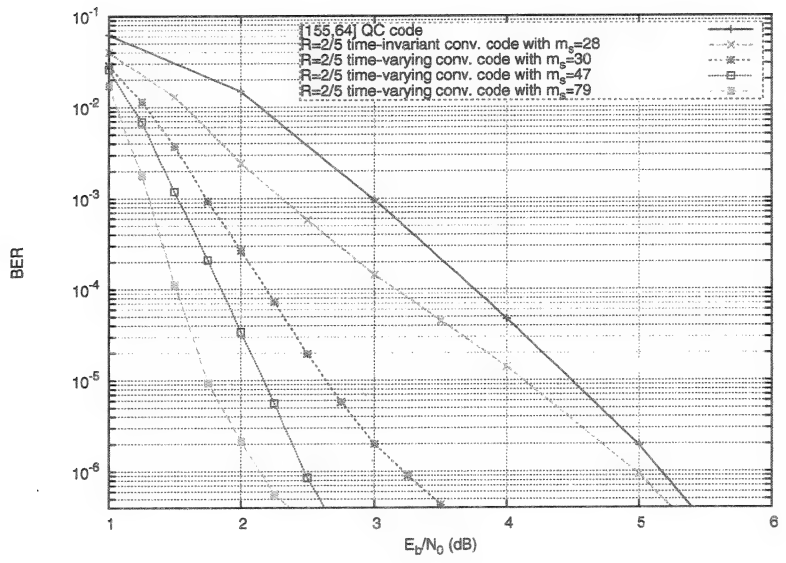

Figure 14. The performance of LDPC convolutional codes derived from quasi-cyclic block LDPC codes.

iterative message passing decoding of the two codes has the same computational and hardware complexity.

In [14], we introduced a new unwrapping technique that results in a time-varying LDPC-CC with significantly improved performance. For the same example noted above, the time-varying unwrapping results in an additional 1.5-2.5dB of "convolutional gain" beyond that achieved by the time-invariant unwrapping! (See Figure 14.) This very surprising result comes from unwrapping the same original QCLDPC-BC, but beginning with a larger circulant size (block length). In other words, the original QCLDPC-BC operates as a kind of protograph from which a whole set of LDPC-CCs with significant "convolutional gain" can be derived.

Further, in [15], we applied the new unwrapping techniques to irregular LDPC-BCs constructed at Caltech's Jet Propulsion Laboratory (JPL). In particular, the [2560, 1024] (rate 2/5) JPL ARA code and the punctured [2048, 1024] (rate 1/2) JPL ARA code were chosen for comparison. Our results show that, with the time-varying unwrapping, the "convolutional gain" is about 1.0dB in the rate 2/5 case and about 0.75dB in the rate 1/2 case. (See Fig. 15.) In addition, we applied the same methods again to the irregular LDPC-BC JPL protograph codes. The protograph codes selected for comparison each had block lengths of about 2500, with code rates ranging from 1/2 to 4/5. Again, using the time-varying unwrapping, "convolutional gains" ranging from 0.6dB to 0.9dB were obtained. (See Figure 15.)

This report briefly summarizes several recently discovered methods by which good LDPC-BCs can be unwrapped to obtain LDPC-CCs with significant "convolutional gains" and es-

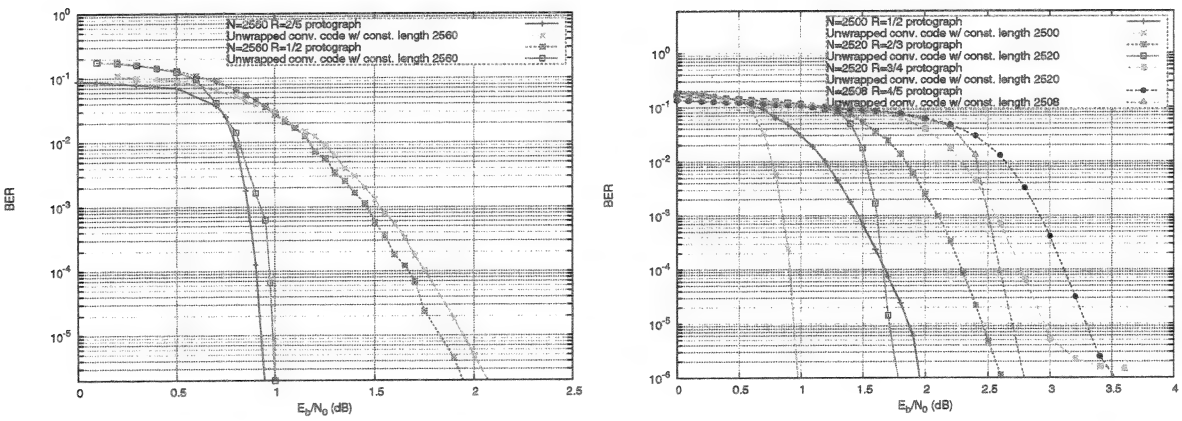

Figure 15. LDPC convolutional codes derived from JPL's ARA-based codes (left) and protograph-based codes (right).

sentially the same decoding complexity. Among the benefits of these LDPC-CCs compared to their LDPC-BC counterparts are the following:

- Substantial "convolutional gains" are obtained with no increase in decoding computational or hardware complexity.
- The codes are well suited for streaming data, since continuous decoding is achieved naturally.
- For framed data, a large variety of frame lengths can be realized with the same code simply by choosing different termination lengths, so there is no need to design separate codes for applications that require multiple frame lengths.
- A natural pipelined decoding architecture can be used to achieve high-speed decoding.
- Low power, small area, and high-speed VLSI implementations with minimal routing congestion can be realized because of the modularity of the decoding graph.
- A simple shift-register based systematic encoding circuit can always be implemented.

Among the disadvantages of LDPC-CCs are the following:

- The improved performance comes at the expense of increased latency, since the decoding graph is extended in time.
- If the same code is used to realize a variety of frame lengths, performance will be suboptimum for some lengths.

- Depending on the code memory, it may be difficult to efficiently realize short frame lengths, due to the rate loss caused by termination.
- VLSI decoder implementations can be quite memory intensive.

Finally, we note that the "convolutional gains" obtained from unwrapping tend to diminish as the size of the original LDPC-BC gets large. This is to be expected, since these codes already operate quite close to capacity.

2.2 Peak-to-Average Power Ratio Reduction for Nyquist-Filtered QPSK Modulation

Consider the root raised-cosine pulse shaped QPSK modulation. We model the pulse shaping filter as a convolutional encoder. The constraint length of the encoder is equal to the truncating length of the filter minus one, and the outputs are the pulse shaped QPSK waveforms for a single symbol duration. Therefore, the total number of states of the convolutional encoder is $4M - 1$, where M is the truncation length of the filter. Some edges of the trellis produce zero-crossing waveforms and some produce peaks. By pruning such edges, i.e., eliminating the state transition that will generate large peak or zero-crossing, we are able to reduce the peak-to-average power ratio (PAPR) significantly.

Simulations have been carried out for pulse shaping filters with a rolloff factor equal to 0, 0.1, 0.2 and 0.3 respectively. In these simulations, the truncating length M is 6 symbols with 10 samples per symbol. PAPR versus pruning percentage is shown in Figure 16.

Assume QPSK modulation over an additive white Gaussian noise (AWGN) channel. X^N is the input sequence with each symbol x^k drawn from the QPSK constellation. Y^N is the AWGN channel output. The mutual information between X^N and Y^N can be calculated numerically using the decision feedback aided BCJR algorithm. The simulation results are shown in Figure 17. At low SNR, the capacity loss due to pruning is very small. Therefore, by choosing an appropriate coding scheme, we can reduce the PAPR of QPSK without much damage to capacity. This pruning method can be extended to all M-ary PSK and M-ary QAM.

2.3 Multilevel Coding for Linear ISI channels

For communication channels affected by intersymbol interference (ISI), we propose a multilevel coding (MLC) scheme with a capacity that approaches the i.i.d. Gaussian input capacity C_{iid} of the ISI channel with linear complexity in channel memory. The transmitter applies MLC and linear mapping, in which M independently encoded binary streams are weighted and summed to produce the sequence of the channel input symbols. The number M of binary streams is large so that the channel input has a Gaussian distribution. A multistage receiver performs separate successive linear minimum mean square error (LMMSE) equalization and

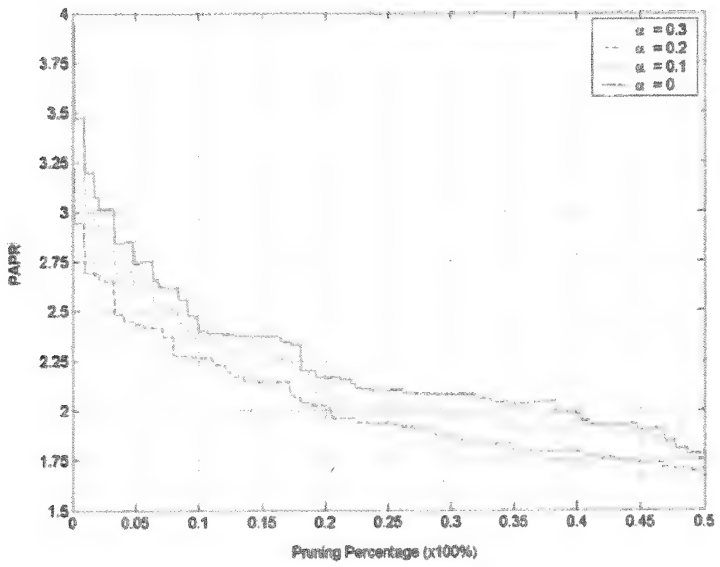

Figure 16. PAPR versus pruning percentage.

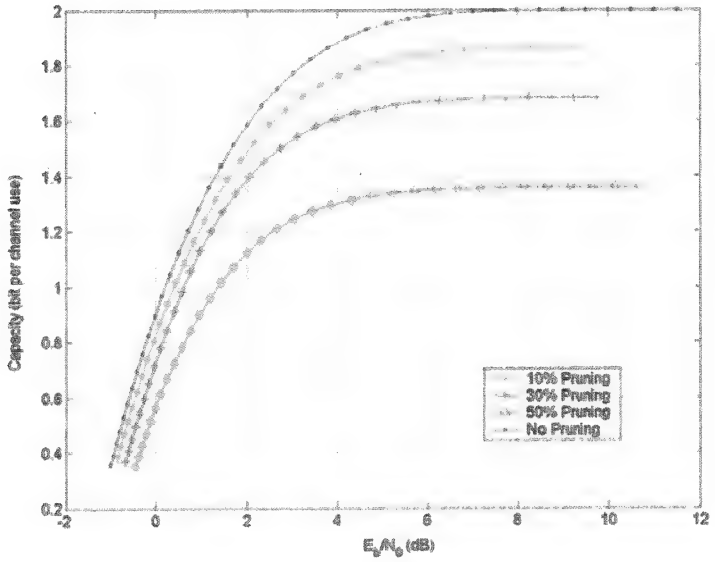

Figure 17. Capacity of unpruned and 10%, 30%, and 50% pruned QPSK modulation assuming an AWGN channel.

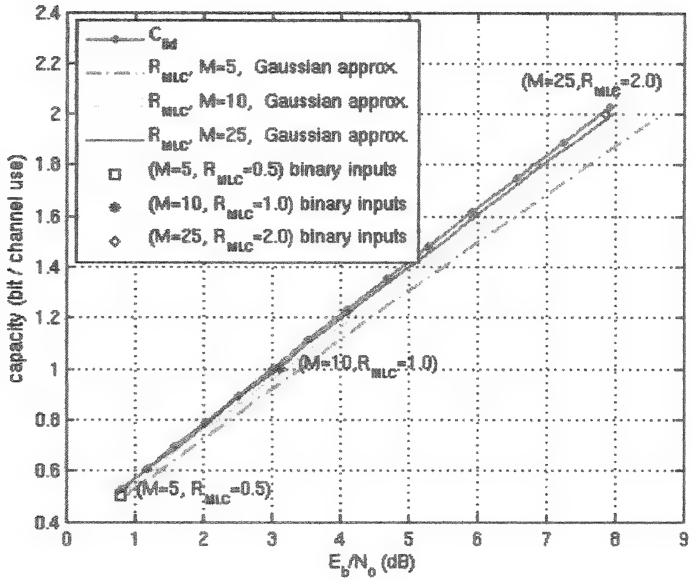

Figure 18. Capacity of unpruned and 10%, 30%, 50% pruned QPSK modulation under an AWGN channel.

decoding on the M streams. Once a stream is decoded, its effect on the channel output can be completely removed. At the same time, all undecoded streams produce a non-white additive Gaussian interference to the current stream being decoded. By making M large, each binary stream operates in a low signal to interference plus noise ratio (SINR) region. More importantly, the LMMSE equalizer is information lossless in this SINR region. The overall system is not only computationally efficient, as the complexity scales linearly with the channel memory L and M, but also optimal. The achievable rate of the MLC scheme with equal rate power allocation, where the power is allocated in such a way that each layer has equal achievable rate, is plotted in Figure 17 together with C_{iid}.

2.4 Adaptive Modulation

Adaptive transmission systems exploit some knowledge about the communication channel to increase the system capacity and/or to enhance the communication link's reliability. Such systems could include a combination of adaptive modulation and coding (AMC), multiple antenna systems including spatial multiplexing and transmit/receive diversity techniques, and multiuser scheduling.

Traditionally, research in this area was focused on the impact of partial or noisy channel state information (CSI) at the receiver in order to compute the throughput and/or BER performance. On the other hand, adaptive transmission techniques require channel state information

at the transmitter (CSIT) for resource allocation. In multiuser systems, each user's CSI is required for user scheduling in order to satisfy some optimality or fairness criterion. AMC systems require CSI to select the appropriate modulation and coding rate that maximize the spectral efficiency. Some transmit diversity and spatial multiplexing systems require CSI to optimize power allocation and transmit precoding, while broadcast systems require CSI for simultaneous transmission to multiple users. As a result, CSI acquisition at the transmitter is an active area of research. The sources of noisy CSI include:

- Modelling errors in the channel fading statistics;
- Feedback delay;
- Channel estimation error;
- Feedback errors on the reverse channel;
- Bandwidth constrained feedback, and
- Quantization error.

Much of the recent research on noisy CSIT has focused on feedback delay, channel estimation error and bandwidth-constrained feedback transmission. In most of the literature on adaptive transmission it has been assumed that the feedback channel itself is error-free. In this research project, we have investigated practical feedback channels that are subject to feedback errors, for both single- and multi-user systems. Our results are summarized below:

1. In our studies on the impact of imperfect feedback channels, we have included fading and additive noise attributes on the feedback channel model considered. We compared the effects of CSI imperfection due to feedback delay, and those due to feedback channel errors. For single-user frequency division duplex (FDD) AMC systems, we concluded that feedback errors usually have a significantly greater impact on system performance (measured by bit-error rate, or BER).

2. We proposed a practical discrete feedback transfer scheme, where system performance now depends on the feedback detection schemes employed. We first analyzed the performance of various feedback detection schemes, including maximum likelihood (ML) and maximum *a posteriori* (MAP) receivers. We formulated the problem as one of a classical multiple hypotheses testing. Conventional wisdom states that the average feedback BER for a MAP receiver is upper-bounded by the average feedback BER for the ML receiver. However, this performance advantage does not carry over to the AMS spectral efficiency and is only true for low to moderate average signal-to-noise ratio (SNR). We also employed the Finite-State Markov Channel (FSMC) model [16] for a slowly fading Rayleigh channel to design feedback receivers. The FSMC-based receiver improves

the performance of ML detection by exploiting the *one-step transition* property of the FSMC model.

3. We extended our investigations on the feedback channel to multi-user scheduling. We showed that feedback error could cause not only erroneous constellation selection, but also erroneous user selection because of quantization error. The coupled effect of quantization and feedback errors leads to an increase in the outage region in the high SNR region.

4. We also investigated the tradeoff that exists between increasing system capacity and the cost of feedback for a multi-user system. We have shown that though multiple users provide another form of diversity in fading channels, the cost of feedback limits the number of users that may be served at any one time. However, less power may be required for training as the number of users increases.

5. In this project, we also considered the antenna selection problem in multiple-input, multiple-output systems. This problem addresses the tradeoff that exists between the spatial diversity benefit of multiple antennas and the cost of radio-frequency (RF) chains. It is concerned with finding the *optimum* subset of RF links in a matrix channel with some specified performance criterion (e.g., capacity). The basic idea is to employ a greater number of antennas compared to the number of RF chains, and then select a subset of these antennas. An optimum solution usually requires an exhaustive search (over all possible combinations of subsets of antennas). We have developed a sub-optimal fast selection algorithm that reduced the search complexity by utilizing the channel's temporal fading statistics, i.e., the channel's memory. The main idea here is that, due to channel memory, at least some of the current optimum subset of antennas will still be in the optimum subset at the next selection. Simulation results showed that our algorithm offers a complexity reduction by a factor of 4 to 6, compared to some existing suboptimum algorithms [17].

2.5 MIMO Processing in OFDM Channels

Orthogonal frequency division multiplexing (OFDM) has gained a great deal of popularity in recent years due to several winning advantages, namely, spectral efficiency, efficient immunity to multipath fading as well as noise, and flexibility in resource allocation. It has been employed in various commercial systems that include wireless local area networks (WLAN/IEEE 802.11a/g/n and HIPERLAN/2), wireless metropolitan area networks (WMAN/WiMax, IEEE 802.16), terrestrial digital audio broadcasting (DAB) and terrestrial digital video broadcasting (DVB) systems.

However, there are some serious drawbacks of OFDM. The most notable ones are high peak-to-average power ratio (PAPR) and sensitivity to synchronization errors. In this part

of the project, we studied the issues related to synchronization errors. We also investigated multiple-input multiple-output (MIMO) OFDM systems including synchronization and interference mitigation.

The synchronization errors of OFDM, which include timing and frequency errors, come from two sources: the local oscillators frequency difference, and the Doppler spread due to the relative motion between the transmitter and the receiver. Both timing and frequency errors introduce extra interference (like inter-channel interference or ICI) to OFDM systems and result in performance degradation. In particular, timing errors have two major effects in OFDM systems: 1) it causes inter-symbol interference (ISI), and 2) it degrades the performance of channel estimation. If the samples contained in one received OFDM symbol are influenced by more than one transmitted OFDM symbol, the demodulated signal will be corrupted by ISI and the orthogonality between subcarriers can also be violated, thereby causing ICI. Both ISI and ICI result in additional disturbance and distortion to the demodulated signal and can lead to significant degradation in system performance. In a coherent OFDM system, timing offset has another, possibly even more severe, impact on system performance, namely, degradation of the performance of channel estimation. When some portions of the effective channel are shifted outside the channel estimation window due to timing offset, the channel estimates will have additional errors. The problem is even more pronounced for some channel estimators that have a narrower estimation window which is matched to the channel impulse response (CIR). Likewise, frequency offset causes ICI and destroys orthogonality among sub-carriers in OFDM systems, resulting in significantly reduced effective signal-to-noise ratio (SNR). Our results are summarized below:

1. We have developed a fine timing synchronization algorithm that employs maximum-likelihood estimation (MLE) method, utilizing estimated channel impulse response (CIR) at the receiver to obtain improved timing performance. The estimated CIR at the receiver is modeled as a complex Gaussian random process parameterized by timing offset. This proposed scheme can be implemented in either integer timing precision or in real-valued timing precision. For the former, the MLE is simplified as a power-delay-profile (PDP)-based correlation scheme. For the latter, it is implemented in a PDP-based delay-locked-loop structure. We have performed theoretical and numerical investigations on the proposed scheme which is shown to offer significantly improved estimation and tracking performance over existing schemes (see, e.g., [18]), measured by the correct estimation probability.

2. Relevant to carrier synchronization, we developed a carrier frequency offset (CFO) estimation scheme based on time-domain channel estimates. We showed that time-domain channel estimates retain quite well the CFO information, exhibited in the form of phase rotation of the estimated channel multipaths. The resulting CFO estimate turns out to be an MLE for the CFO. Incorporating the Doppler effect of the fading channel, the

proposed CFO MLE is shown to achieve significant performance gain over existing schemes such as [19, 20] with reduced complexity. The complexity reduction results from the fact that the proposed estimation schemes work on the time-domain channel estimate whose length is much shorter than a typical FFT size in OFDM. Furthermore, the proposed CFO estimator does not require a specific pilot pattern (like some schemes require consecutive pilot symbols to be identical).

3. We have extended the CFO estimation scheme to MIMO-OFDM. Note that, for MIMO systems, the power of additional noise due to synchronization errors increases linearly with the number of transmitters. Furthermore, the interference due to synchronization errors in different diversity branches of the receiver originating from the same transmitted symbols is correlated. This correlated interference, unlike the channel noise, can not be necessarily abated by the receiver diversity. Thus its impact on MIMO decoding becomes more severe (comparing to the impact of channel noise) as the number of the receiver antennas increases. Our extended scheme also enjoys improved synchronization performance with reduced complexity.

4. In addition to the above investigations on synchronization issues, we also developed an OFDM-based multi-user broadcast scheme that features optimum subchannel and user allocation (based on instantaneous channel conditions). In our scheme, assuming that the CSI is known, the subset of users for each subcarrier and the transmit beamforming vector are optimized (subject to the transmit power constraint) which effectively mitigated CCI and significantly increased the data throughput rate over existing schemes that either assigns one subcarrier to only one user or assign each subcarrier to all users, see, e.g., [21, 22]. The proposed scheme efficiently exploits the wireless channels through optimal user and subcarrier allocation according to the time-varying nature of radio channels and multi-user diversity.

3 Development of the Wireless at Notre Dame (WAND) Lab

Finally, we observe that a significant amount of the funding provided under award DAAD16-02-C-0057 was used to enhance and upgrade the Wireless at Notre Dame (WAND) laboratory. Among the equipment items purchased with funding from this award were:

- An Agilent E4438C vector signal generator;
- Two Agilent E4440A spectrum analyzers and an Agilent E8251A signal generator;
- An HP 3589A spectrum/network analyzer;
- Two Tektronix WCA280A wireless communication analyzers;

- A Tektronix AWG430 arbitrary waveform generator;
- A Tektronix TDS7104 digital oscilloscope and an HP 54503A digital oscilloscope.

This document reports research undertaken at the U.S. Army Natick Soldier Research, Development and Engineering Center, Natick, MA, and has been assigned No. NATICK/TR-08/1004 in a series of reports approved for publication.

This page intentionally left blank.

References

[1] P. C. Massey, "A 4-state alternative code to the proposed 8-state turbo coding standard," in *IEEE Communiation Theory Workshop*, Borrego Springs, CA, May 2001.

[2] P. C. Massey and D. J. Costello Jr., "New low-complexity turbo-like codes," in *Proceedings of the IEEE Information Theory Workshop*, Cairns, Australia, Sept. 2001, pp. 70–72.

[3] K. M. Chun-Hsuan Kuo and K. Chugg, "On the bandwidth efficiency of CPM signals," MILCOM 2004, vol. 1, pp. 218-224, November 2004.

[4] K. M. Chun-Hsuan Kuo and K. Chugg, "Improving the bandwidth efficiency and performance of CPM signals via shaping and iterative detection," MILCOM 2005, vol. 2, pp. 1162-1166, October 2005.

[5] A. Salehi, "Frequency-independent and frequency-dependent nonlinear models of TWT amplifiers," *IEEE Transactions on Communications,* vol. 29, no. 11, pp. 1715-1720, November 1981.

[6] A. Schaefer, A. Sridharan, M. Moerz, J. Hagenauer, and D. J. Costello, Jr., "Analog rotating ring decoder for an LDPC convolutional code," in *Proc. IEEE Inform. Theory Workshop*, (Paris, France), pp. 226–229, April 2003.

[7] A. Sridharan, D. Truhachev, M. Lentmaier, D. J. Costello, Jr., and K. Sh. Zigangirov, "On the free distance of LDPC convolutional codes," in *Proc. IEEE Intl. Symposium on Inform. Theory*, (Chicago, IL, USA), p. 311, June 2004.

[8] A. Sridharan, M. Lentmaier, K. Sh. Zigangirov, and D. J. Costello, Jr., "Convergence analysis of LDPC convolutional codes on the erasure channel," in *Proc. 42nd Allerton Conference on Communication Control, and Computing*, (Monticello, Illinois, USA), pp. 685–689, Sept. 2004.

[9] M. Lentmaier, D. V. Truhachev, K. Sh. Zigangirov, and D. J. Costello, Jr., "An analysis of the block error probability performance of iterative decoding," *IEEE Trans. Inform. Theory*, to appear.

[10] A. Schaefer, A. Sridharan, B. Koenig, and D. J. Costello, Jr., "Decoder implementation issues for low-density parity-check convolutional codes," in *Proc. Intl. Symposium on Information Theory and its Applications*, (Parma, Italy), pp. 194–199, Oct. 2004.

[11] A. Sridharan, D. Truhachev, M. Lentmaier, D. J. Costello, Jr., and K. Sh. Zigangirov, "Distance bounds for a class of LDPC convolutional codes constructed from permutation matrices," *submitted to IEEE Trans. Inform. Theory*, Jan. 2005.

[12] A. Sridharan, M. Lentmaier, K. Sh. Zigangirov, and D. J. Costello, Jr., "Terminated LDPC convolutional codes with thresholds close to capacity," in *Proc. IEEE Intl. Symposium on Inform. Theory*, (Adelaide, Australia), pp. 1372–1376, September 2005.

[13] R. M. Tanner, D. Sridhara, A. Sridharan, T. E. Fuja, and D. J. Costello, Jr., "LDPC block and convolutional codes based on circulant matrices," *IEEE Trans. Inform. Theory*, vol. IT-50, pp. 2966–2984, Dec. 2004.

[14] A. E. Pusane, R. Smarandache, P. O. Vontobel, and D. J. Costello, Jr., "On deriving good LDPC convolutional codes from QC LDPC block codes," *submitted to IEEE Intl. Symp. on Inform. Theory*, Jan. 2007.

[15] D. J. Costello, Jr., A. E. Pusane, C. R. Jones, and D. Divsalar, "A comparison of ARA- and protograph-based LDPC block and convolutional codes," in *Proc. Information Theory and Applications Workshop*, (San Diego, CA, USA), January 29-February 2, 2007.

[16] H.S. Wang and N. Moayeri, "Finite-state Markov channel - a useful model for radio communication channels," *IEEE Transactions on Vehicular Technology*, Vol. 44, No. 1, pp. 163-171, February, 1995.

[17] A. Gorokhov, D. a. Gore, and A.J. Paulraj, "Receive antenna selection for MIMO spatial multiplexing: theory and algorithms," *IEEE Transactions on Signal Processing*, Vol. 51, No. 11, pp. 2796-2807, November, 2003.

[18] N. Chen, M. Tanaka, and R. Heaton, "OFDM timing synchronization under multi-path channels," *IEEE Vehicular Technology Conference*, Vol. 1 pp. 378382, April, 2003.

[19] Paul H. Moose, "A technique for orthogonal frequency division multiplexing frequency offset correction," *IEEE Transactions on Communications*, Vol. 42, No. 10, pp. 29082914, October 1994.

[20] P. Y. Tsai, H. Y. Kang, and T. D. Chiueh, "Joint weighted least-squares estimation of carrier-frequency offset and timing offset for OFDM systems over multipath fading channels," *IEEE Transactions on Vehicular Technology*, Vol. 54, No. 1, pp. 211223, January, 2005.

[21] L. Q. Hoo, B. Halder, J. Tellado, and J. M. Cioffi, "Multiuser transmite optimization for multicarrier broadcast channels: asymptotic FDMA capacity region and algorithm," *IEEE Transactions on Communications*, Vol. 52, No. 6, pp. 922 930, June 2004.

[22] J. Duplicy, J. Louveaux, and L. Vandendorpe, "Interference-free multi-user MIMO-OFDM," in *IEEE International Conference on Acoustics, Speech, and Signal Processing*, Vol. III, pp. 1149 1152, March 18-23, 2005.